

Construction of Maximally Localized Wannier Functions

Junbo Zhu,¹ Zhu Chen,² and Biao Wu^{1, 3, 4, 5, *}

¹*International Center for Quantum Materials, School of Physics, Peking University, Beijing 100871, China*

²*Institute of Applied Physics and Computational Mathematics, Beijing 100088, China*

³*Collaborative Innovation Center of Quantum Matter, Beijing 100871, China*

⁴*Wilczek Quantum Center, College of Science, Zhejiang University of Technology, Hangzhou 310014, China*

⁵*Synergetic Innovation Center for Quantum Effects and Applications (SICQEA),*

Hunan Normal University, Changsha 410081, China

(Dated: September 17, 2022)

We present a general method of constructing maximally localized Wannier functions. It consists of three steps: (1) picking a localized trial wave function, (2) performing a full band projection, and (3) orthonormalizing with the Löwdin method. Our method is capable of producing maximally localized Wannier functions without further minimization, and it can be applied straightforwardly to random potentials without using supercells. The effectiveness of our method is demonstrated for both simple bands and composite bands.

PACS numbers: 71.23.An, 71.15.-m, 72.80.Ng, 37.10.Jk

Wannier functions that are localized at lattice sites are an alternative representation of electronic states in crystalline solid to the Bloch wave representation [1]. They offer an insightful picture of chemical bonds, play a pivotal role in the modern theory of polarization [2, 3], and are the basis for an efficient linear-scaling algorithms in electric-structure calculations [4, 5]. Wannier functions are also important in linking cold atom experiments in continuous light potentials with lattice Hamiltonians, such as the Bose-Hubbard model and Anderson random lattice [6–8].

Although there are explicit formula that transform Bloch waves to Wannier functions, the construction of Wannier functions is far from trivial. The primary reason is that there are infinite number of Wannier functions for a given band due to phase choices for Bloch waves whereas in practice the maximally localized Wannier functions (MLWFs) are sought and preferred [9]. For one dimensional lattice, Kohn showed how to fix the Bloch wave phases to obtain these MLWFs [10]. In 1971, Teichler found a general method to construct Wannier functions, which is insensitive to the phases of Bloch waves [11]. However, this method does not guarantee maximal localization and depends on initial trial function. A more sophisticated method involving numerical minimization of the spread of a Wannier function has been developed to compute MLWFs [12]. There are also some new developments recently [13–15].

In this work we present a general method for computing MLWFs. Our method is somehow similar to Teichler’s method as it also involves projection and the Löwdin orthonormalization method [16]. Nevertheless there is a significant difference so that our method can produce MLWFs and is insensitive to the initial trial wave functions. Compared to the method in Ref. [12], our method does not need the minimization procedure. As our method uses the full band projection, it can be ap-

plied straightforwardly to random potential without using supercells. The effectiveness of our method is demonstrated for both simple bands and composite bands.

We consider a simple band that is isolated from other bands. Composite bands will be discussed later. Our method of constructing MLWFs consists of three steps:

1. Guess: choose a set of trial wave functions $|g_n\rangle$, which are localized at lattice sites.
2. Projection: $|\xi_n\rangle = P|g_n\rangle$, where $P = \sum_k |\psi_k\rangle\langle\psi_k|$ with the summation over the whole first Brillouin zone. Note that P is a full band projection and is different from the projection in Refs. [9, 11], which is at a given k point. As a result of this crucial difference, the projected function $|\xi_n\rangle$ is localized at site n .
3. Orthonormalization: use the Löwdin orthonormalization method [16] to transform $|\xi_n\rangle$ into a set of MLWFs $|w_n\rangle$. If one uses other methods such as Kohn’s method [17] to orthonormalize $|\xi_n\rangle$, the resulted Wannier function is unlikely maximally localized.

Here is why our method is effective and capable of producing MLWFs. We re-write the full band projection operator in terms of Wannier functions, $P = \sum_n |w_n\rangle\langle w_n|$, where the summation is over all lattice sites. We thus have

$$|\xi_n\rangle = \sum_m |w_m\rangle\langle w_m|g_n\rangle \approx \sum_{m=\langle n \rangle} |w_m\rangle\langle w_m|g_n\rangle, \quad (1)$$

where $\langle n \rangle$ indicates that the summation is only over site n and its nearest neighbors. It is clear that $|\xi_n\rangle$ is localized at lattice site n . However, these projected functions $|\xi_n\rangle$ ’s are not orthonormal. Any orthonormalization of $|\xi_n\rangle$ ’s will give us a set of Wannier functions. For example, one

may use Kohn's method [17]. We choose the Löwdin method [16] as it can produce the MLWFs. According to Ref. [18], the Löwdin orthogonalization uniquely minimizes the functional measuring the least squares distance between the given orbitals and the orthogonalized orbitals. In our case, for the set of projected orbitals $|\xi_n\rangle$, the Löwdin method produces Wannier functions $|w_n\rangle$ that minimize

$$\sum_n \int dx |\langle x|\xi_n\rangle - \langle x|w_n\rangle|^2, \quad (2)$$

where the summation is over all lattice sites. For a periodic potential, this is equivalent to maximizing $\langle w_n|\xi_n\rangle = \langle w_n|g_n\rangle$. Therefore, if $|g_n\rangle$ is properly chosen, the resulted Wannier function is maximally localized. No further minimization such as the one in Ref. [12] is needed.

To illustrate our method, we consider a single particle Hamiltonian with the periodic potential $V(x) = \cos(2\pi x/a)$, where a is the lattice constant. We construct the Wannier function for its lowest band. As each potential well is symmetric with respect to its center (the lowest point of the well), we expect that the MLWF is also symmetric with its highest peak at the center. So, we choose $\langle x|g_n\rangle = e^{-(x-na)^2/2a^2}/\sqrt{2\alpha^2\pi}$. It is clear that $\langle w_n|g_n\rangle$ is the largest for a narrowest Wannier function allowed within the band or MLWF. The resulted Wannier function should be insensitive to the width of $\langle x|g_n\rangle$. This is exactly what we see in Fig. 1(a). With three Gaussians of different widths $\alpha = a, 0.5a, 0.1a$ as trial functions, the resulted Wannier functions fall right on top of each other as seen in Fig. 1(a). We have computed the spread of the Wannier functions obtained with our method; they are almost identical for Gaussian trial functions of different widths as seen Fig. 1(b).

To further illustrate the effectiveness of our method, we have computed Wannier functions with two other methods. One is the traditional method, where one fixes the phases of the Bloch waves according to the prescription in Ref. [10]. The other method is to orthonormalize $|\xi_n\rangle$'s with Kohn's method [17]. They are compared to our results in Fig. 1(c), where we see that our result is in excellent agreement with the traditional method while the one obtained with Kohn's method is much worse.

The Löwdin method can be implemented differently. However, as long as it is implemented correctly, the method transforms a given set of non-orthogonal vectors to a unique set of orthonormal vectors. Nevertheless, we show here explicitly how we implement it. We impose a periodic boundary condition with N unit cells. As a result, the crystal wave vector k takes N discrete values k_1, k_2, \dots, k_N . We let $|\psi_j\rangle = |\psi_{k_j}\rangle$ and $A_{nj} = \langle \psi_j|g_n\rangle$. The Löwdin orthonormalization is then implemented as

$$|w_n\rangle = \sum_{mj} (AA^\dagger)^{-1/2}_{nm} A_{mj} |\psi_j\rangle. \quad (3)$$

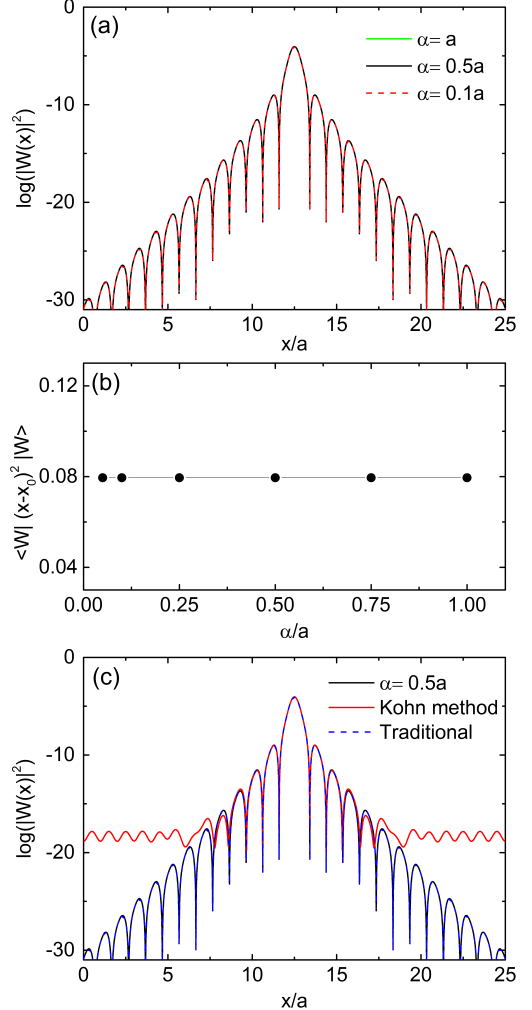


FIG. 1: (color online) Wannier functions for one dimensional periodic potential $V(x) = \cos(2\pi x/a)$. (a) The Wannier functions obtained with our method with trial Gaussian functions of different widths α . (b) The spread of the Wannier function obtained with our method as a function of the width of the Gaussian function α . (c) The Wannier functions obtained with three different methods. The black line is our method; the blue line is obtained with the traditional method, where one fixes the phases of Bloch wave according to the prescription given in Ref. [10]; the red one is obtained by orthonormalizing $|\xi_n\rangle$'s with Kohn's method [17].

If the trial function $|g_n\rangle$ is translationally symmetric, $\langle x|g_n\rangle = \langle x-r_n|g_0\rangle$, we have $A_{nj} = e^{-ik_j r_n} A_{0j}$ and $(AA^\dagger)_{nm} = \sum_j e^{ik_j(r_m-r_n)} |\langle \psi_j|g_0\rangle|^2$.

Our method is applicable for composite bands. In composite bands, one or more Wannier functions have nodes. Therefore, to have largest $\langle w_n|g_n\rangle$ for MLWFs, we need to choose such $|g_n\rangle$'s that they have nodes at proper positions. The node positions can be determined by symmetries of the wells. In the worst case, we can determine these node positions by numerically

computing the eigenstates of the local wells. Here we consider a two dimensional periodic potential $V(x, y) = V_0[\cos(2\pi x/a) + \cos(2\pi y/a)]$ and use its p-bands to illustrate the effectiveness of our method for composite bands. The two trial wave functions are chosen as $g_{1,2} = \sqrt{\frac{\pi}{2\alpha^4}}\eta_{1,2}e^{-(x^2+y^2)/2\alpha^2}$ with $\eta_1 = x, \eta_2 = y$, which are the two first excited states of a two dimensional harmonic oscillator. The results are plotted in Fig.2. Shown in Fig.2(a) is a comparison between the trial function and the resulted Wannier function. Three Wannier functions obtained from different trial functions are shown in Fig.2(c) and (d). Our numerical calculations show that when the width of the trial function α is narrow enough, the resulted Wannier functions are almost identical to each other. When they are plotted in the figure, they fall right on top of each other. So, in Fig.2(c) and (d) only three Wannier functions are plotted. The spread of a Wannier function $\langle w|x^2+y^2|w\rangle$ is plotted as the function of α in Fig.2(b), which shows that the Wannier function spread no longer changes when α is narrow enough.

Our method is directly applicable to random potentials. The reason is that we use the full band projection. It can be constructed with all the energy eigenfunctions in a given band no matter the eigenfunctions are Bloch waves or not. It is well known that even in random potentials, there exist eigen-energy “band” that are isolated from other eigen-energies by gaps that are independent of the system size. For these bands, there exist Wannier functions [19]. Our method can be used to compute these Wannier functions by constructing the projection P with the energy eigenstates of a given random energy band. According to Eq.(2), the resulted Wannier functions maximize a sum, $\sum_n \langle w_n | g_n \rangle$. With a proper choice of $|g_n\rangle$ ’s, these Wannier functions can be regarded as maximally localized collectively. There already exist several methods to compute Wannier functions for random potentials. Our method has various advantages. The method in Ref. [20] is only applicable to the case where the random potential is a perturbation to a periodic potential. Kivelson’s method [21] has difficulty for two or three dimensional systems. Our method is clearly more efficient than the one in Ref. [8]. We ourselves have recently proposed a method to compute Wannier functions for random potentials [22]. Our current method is certainly superior.

We now illustrate our method in disordered systems. We choose a disordered potential as a series of cosine-type wells of random depths, $V_n(x) = A_n[\cos(2\pi x/a) - 1]$. Well depths $A_n = A[1 + \eta \cdot \mathfrak{R}_n]$, where A is a constant and \mathfrak{R}_n denotes a sequence of random numbers between -0.5 and 0.5, and η denotes the relative strength of disorder. For instance, we refer to $\eta = 0.1$ as a 10% disorder. We use $A = 5$ and $a = 1$, and $\eta = 0.3$ in the example shown in Fig. 3. In our computation, we choose the Gaussian trial functions $|g_n\rangle$ for different wells despite the wells are different. As shown in Fig. 3, our method produces suc-

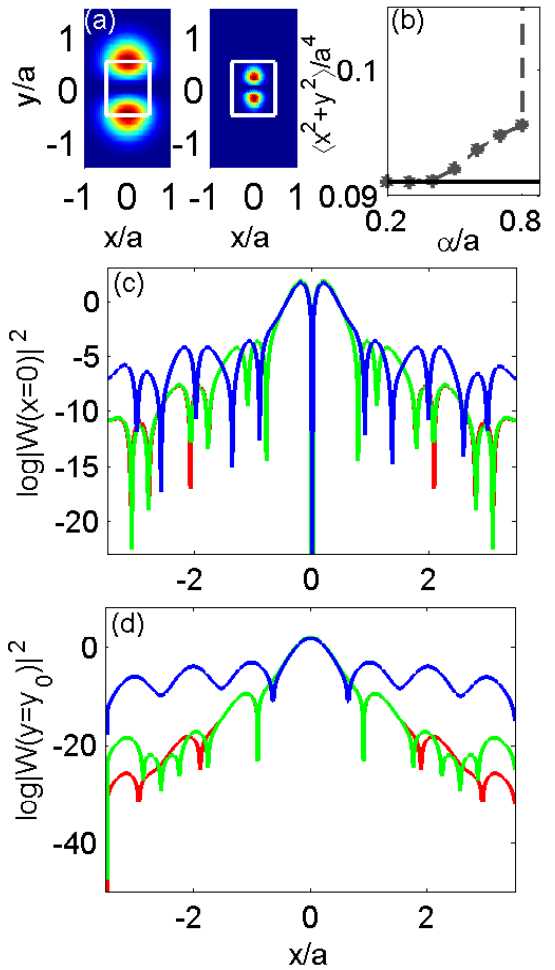


FIG. 2: (color online) Wannier functions of the composite p-bands in a two dimensional lattice $V(x, y) = V_0[\cos(2\pi x/a) + \cos(2\pi y/a)]$ with $V_0 = -30$. (a) The left is the trial wave function g_2 with $\alpha = 0.5a$; the right is the Wannier function obtained with this trial function. The white dashed line marks the unit cell. (b) The spread $\langle w|x^2+y^2|w\rangle$ of a Wannier function with respect to varying α . The convergence to the black line is obvious. The black line is the width of the Wannier function $w(x, y) = w_1(x)w_2(y)$, where $w_1(x)$ as the s-band Wannier function of $\cos(2\pi x/a)$ and $w_2(y)$ as the p-band Wannier function of $\cos(2\pi y/a)$ are obtained with the traditional method. (c) Logarithmic plot of Wannier functions at $x = 0$ along y -axis for different values of α : $\alpha = 0.3a$ (red), $0.6a$ (green), $0.88a$ (blue). Note that the latter two almost overlap. (d) Logarithmic plot of Wannier functions at y_0 along the x -axis for different choices of α : $\alpha = 0.3a$ (red), $0.6a$ (green), $0.88a$ (blue). y_0 is the highest peak position of the Wannier functions.

cessfully exponentially localized Wannier functions. It is clear that a narrower trial Gaussian function leads to more localized Wannier functions. Numerical results indicate that Gaussian trial functions with σ as small as $0.5a$ is enough to construct MLWFs.

Note that we have so far assumed that the system has

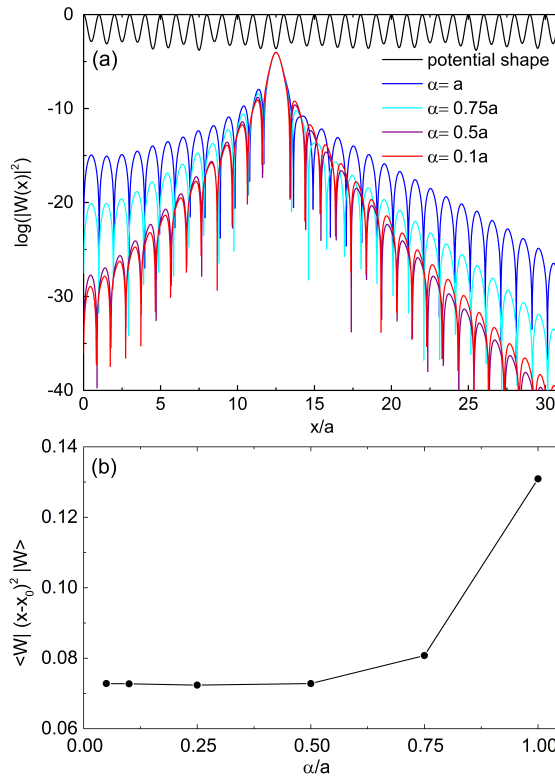


FIG. 3: (color online) Wannier functions constructed by our method for one dimensional 30% disordered potential, which is plotted as the black line at the top of (a). The initial trial Gaussian functions are the same for different wells. (a) The Wannier functions obtained with Gaussian functions of different widths α . (b) The spread of the Wannier functions obtained with our method as a function of the width of the trial Gaussian function.

time reversal symmetry. For these systems, its energy eigenfunctions can always be made real. It follows that the projection P and all the matrices involved in the Löwdin method (Eq.3) can also be made real. Therefore, the final Wannier functions $|w_n\rangle$ are also real as long as the trial functions are real. For systems where the time reversal symmetry is broken, $|w_n\rangle$ can be complex. In this case, the Löwdin method maximizes $\text{Re}\{\langle w_n | g_n \rangle\}$ and we may not obtain MLWFs. We shall leave it for future discussion.

In sum, we have presented a simple and general method for constructing MLWFs. In our method, the full band projection is used on localized trial wave functions. If the trial functions are properly chosen to respect the lo-

cal potential configuration and have good node positions, the ensuing Löwdin method orthonormalize them to MLWFs. No numerical minimization is needed. Our method can be directly applied to random potentials. The application of our method to a real material is left for future.

We thank Ji Feng and Xianqing Lin for helpful discussion. This work is supported by the National Basic Research Program of China (Grants No. 2013CB921903 and No. 2012CB921300) and the National Natural Science Foundation of China (Grants No. 11274024, No. 11334001, and No. 11429402).

* Electronic address: wubiao@pku.edu.cn

- [1] G. H. Wannier, Phys. Rev. **52**, 191 (1937).
- [2] R. Resta, Rev. Mod. Phys. **66**, 899 (1994).
- [3] R. D. King-Smith and D. Vanderbilt, Phys. Rev. B **47**, 1651 (1993).
- [4] S. Goedecker, Rev. Mod. Phys. **71**, 1085 (1999).
- [5] G. Galli, Current Opinion in Solid State and Materials Science **1**, 864 (1996).
- [6] D. Jaksch, C. Bruder, J. I. Cirac, C. W. Gardiner, and P. Zoller, Phys. Rev. Lett. **81**, 3108 (1998).
- [7] M. White, M. Pasienski, D. McKay, S. Q. Zhou, D. Ceperley, and B. DeMarco, Phys. Rev. Lett. **102**, 055301 (2009).
- [8] S. Q. Zhou and D. M. Ceperley, Phys. Rev. A **81**, 013402 (2010).
- [9] N. Marzari and D. Vanderbilt, Phys. Rev. B **56**, 12847 (1997).
- [10] W. Kohn, Phys. Rev. **115**, 809 (1959).
- [11] H. Teichler, Phys. Status Solidi B **43**, 307 (1971).
- [12] N. Marzari, A. A. Mostofi, J. R. Yates, I. Souza, and D. Vanderbilt, Rev. Mod. Phys. **84**, 1419 (2012).
- [13] H. D. Cornean, I. Herbst, and G. Nenciu, arXiv:1506.07435 (2015).
- [14] J. I. Mustafa, S. Coh, M. L. Cohen, and S. G. Louie, arXiv:1508.04148 (2015).
- [15] E. Cancès, A. Levitt, G. Panati, and G. Stoltz, arXiv:160507201 (2016).
- [16] P. Löwdin, The Journal of Chemical Physics **18**, 365 (1950).
- [17] W. Kohn, Phys. Rev. B **7**, 4388 (1973).
- [18] J. G. Aiken, J. A. Erdos, and J. A. Goldstein, International Journal of Quantum Chemistry **18**, 1101 (1980).
- [19] A. Nenciu and G. Nenciu, Phys. Rev. B **47**, 10112 (1993).
- [20] W. Kohn and J. R. Onffroy, Phys. Rev. B **8**, 2485 (1973).
- [21] S. Kivelson, Phys. Rev. B **26**, 4269 (1982).
- [22] J. Zhu, Z. Chen, and B. Wu, arXiv:1512.02043 (2015).